RESEARCH PAPER

Determination of genesis by using geochemical and isotopic studies of iron and oxygen in magnetite ore in the Gol-e-Gohar iron ore district, Sanandaj-Sirjan zone, Iran

Narges Alibabaie [1, *], Dariush Esmaeily [1], Shojaeddin Nirooamand [1], Teymoor Mansouri [2], Bernd Lehmann [3]

[1] School of Geology, College of Sciences, University of Tehran, Tehran, Iran
[2] Gohar-Zamin mine, 55 km. Shiraz Road, 78185-111 Sirjan, Kerman, Iran
[3] Mineral Resources, Technical University of Clausthal, Adolph-Roemer-Strasse 2a, 38678 Clausthal-Zellerfeld, Germany

Abstract
The Gol-e-Gohar iron deposit in the Sanandaj-Sirjan zone of south-western Iran comprises six major ore bodies. The largest deposit is Gol-e-Gohar No. 3 (Gohar-Zamin) with about 643 Mt @ 53.1% Fe. Magnetite is formed in massive and brecciated shapes. Gol-e-Gohar magnetite contains Mg, Ca, and Si up to the percent range, V and Ti in the 100s ppm level, and low Cr, Co, Ni in the tens of ppm range, typical of Kiruna mineralization (especially Bafq mining district). But Chador-Malu magnetite is formed at a higher temperature than Gol-e-Gohar magnetite, therefore, both deposits have the magmatic-hydrothermal high-T nature (magmatic ore-forming fluids), which are related to felsic magmatism (host meta-granites), and both of them are attributed to the Early Paleozoic. The oxygen isotope composition of magnetite is 4.9 ± 0.7‰ $\delta^{18}O$ (n = 9) and the iron isotope composition is 0.49 ± 0.05‰ $\delta^{56}Fe$ (n = 17). These data suggest that the magnetite ore formed from a magmatic-hydrothermal (high-T) fluid in equilibrium with a granitic source. The Gol-e-Gohar iron ore district shows several similarities to the Bafq mining district, located about 400 km to the north, and seems to be a disrupted member of the Kashmar-Kerman arc. Finally, according to the mentioned evidence and comparison of Gol-e-Gohar iron deposit with global samples, the genesis of mineralization in this deposit is most similar to Kiruna-type (Kiruna-type magnetite ± apatite mineralization).

Introduction

Iran has numerous important Kiruna-type (magnetite-apatite) iron ore deposits. The major mining district is in the Kashmar-Kerman arc, i.e., the Bafq mining district with the Choghart, Chador-Malu, Se-Chahun, and Esfordi mines (total resource of about 2 Gt iron ore), and the second district is the Gol-e-Gohar mining area in the SSZ (total resource of about 1135 Mt iron ore). The SSZ is one of the most important metallogenic belts in Iran and has a basement of predominantly medium to high-grade metamorphic rocks of Neoproterozoic age (e.g., gneiss, amphibolite, marble and schist). These rocks are largely covered by complexly deformed Paleozoic and Mesozoic meta-sedimentary and meta-volcanic rocks, which were intruded by

felsic plutons related to the northward subduction of the Tethys Ocean. There is both Middle to Late Triassic folding and metamorphism, and Late Cretaceous tectonic overprint in this belt (Mohajjel et al., 2003; Sheikholeslami et al., 2008). Both districts have a similar setting in Neoproterozoic/Early Cambrian igneous rocks and carbonate rocks with relics of evaporites, but the Gol-e-Gohar iron deposit is more affected by tectonometamorphic overprint and younger episodes of felsic magmatism.

Gol-e-Gohar mining area is located 53 km southwest of Sirjan city and in the geographical position of 29° 03' (latitude) and 24°15´ - 55° 24´ (longitude). The Gol-e-Gohar iron deposit is one of the most important iron deposits in Iran and the world. It is located in the Sanandaj-Sirjan structural zone. So far, various theories have been proposed regarding the genesis of the deposit, including: sediment-chemical genesis (Young, 1976), magmatic-hydrothermal (Mücke & Golestaneh, 1982), Mint and Clinton sedimentary (Evans &Frost, 1975). Sedimentary-volcanic (Hallaji, 1991), sedimentary, Rapitan (Babaki and Aftabi, 2007), Paleo-skarn (Torabian, 2007), Polyphase model affected by sedimentary-volcanic processes that then formed as skarn (Bayati Rad et al., 2010), Sedimentary-Rapitan (Vafaei, 2016) and finally the dual magmatic-hydrothermal and skarn origin (Mirzaei et al., 2018).

Whereas there have been many contradictions in previous studies and in none of them has a comprehensive geochemical and isotopic study on magnetite; Therefore, in this study, all the above evidences are examined to determine the genesis of Gol-e-Gohar iron ore deposit in the Sanandaj-Sirjan structural zone. The study area includes NO.3 anomaly of Gol-e-Gohar, Sirjan (Goharzamin mine). The main objective of the present study is to better understand the genesis of magnetite mineralization at the Gol-e-Gohar iron deposit by using magnetite geochemistry and stable isotope evidence (iron and oxygen isotopes), and comparison with similar deposits in Iran and elsewhere. The location of the most important iron ore mining districts from elsewhere in Iran is shown in the Structural map of Iran (fig. 1).

Geological setting

The Gol-e-Gohar iron deposit is located at the south-eastern margin of the SSZ, about 55 km southwest of the town of Sirjan (Kerman province; Fig. 2). The SSZ is one of the most important structural zones which includes some metallogenic belts such as MEMB, KKA (Kashmar-Kerman Arc, Fig. 1) and etc.

This zone has a basement of predominantly medium to high-grade metamorphic rocks of Neoproterozoic age (e.g., gneiss, amphibolite, marble, and schist). These rocks are largely covered by complexly deformed Paleozoic and Mesozoic meta-sedimentary and meta-volcanic rocks, which were intruded by felsic plutons related to the northward subduction of the Tethys Ocean. There is both Middle to Late Triassic folding and metamorphism, and Late Cretaceous tectonic overprint in this belt (Mohajjel et al., 2003; Sheikholeslami et al., 2008). The Gol-e-Gohar iron deposit includes Late Neoproterozoic / Paleozoic metamorphic rocks in the south and south-west, and sedimentary Mesozoic and Cenozoic rocks in the north and east, which are mostly covered by young Quaternary alluviums. The Late Neoproterozoic/Paleozoic rocks are representative of the Gol-e-Gohar complex (Safarzade et al., 2016). This complex consists of a set of serpentinite ultramafic rocks, meta-gabbros, dolomitic marble and meta-granitic rocks (Mohajjel et al., 2003), which are of low-grade regional metamorphism locally up to upper amphibolite facies due to thermal overprint during the Mesozoic (Fig. 2). Based on U-Pb zircon dating the possible age of the granitic magmatism was estimated between 539 and 581 Ma, i.e., Late Neoproterozoic–Early Cambrian (Safarzade et al., 2016). Similar ages were obtained on metagranitic rocks from other parts of the SSZ and indicate the presence of a Precambrian basement and continental-margin magmatism related to Paleo-Tethys subduction along the entire SSZ (Safarzade et al., 2016) and along the Kashmar-Kerman volcanoplutonic arc, as a

portion of the Central Iranian microcontinent (Ramezani and Tucker, 2003). The Gol-e-Gohar iron deposit contains six ore bodies discovered during magnetic surveys, and first identified by Iran Barite Mining Company in 1969. There are several studies about the genesis of the Gol-e-Gohar iron deposits with different conclusions. Young (1976), Hallaji (1991), Babaki & Aftabi (2006) and Badavi et al. (2019) suggested a marine chemical-sedimentary or volcano-sedimentary origin, while Mücke & Golestaneh (1982) first proposed a magmatic-hydrothermal origin. A paleo-skarn model was applied by Torabian (2007), and a combined model with both volcano-sedimentary iron enrichment and later skarn-type magmatic overprint processes was proposed by Bayati-Rad et al. (2013). Recently, Mirzaei et al. (2018) proposed a model of magmatic-hydrothermal ore formation for this district. The total reserves of the ore bodies are estimated at 1135 Mt.
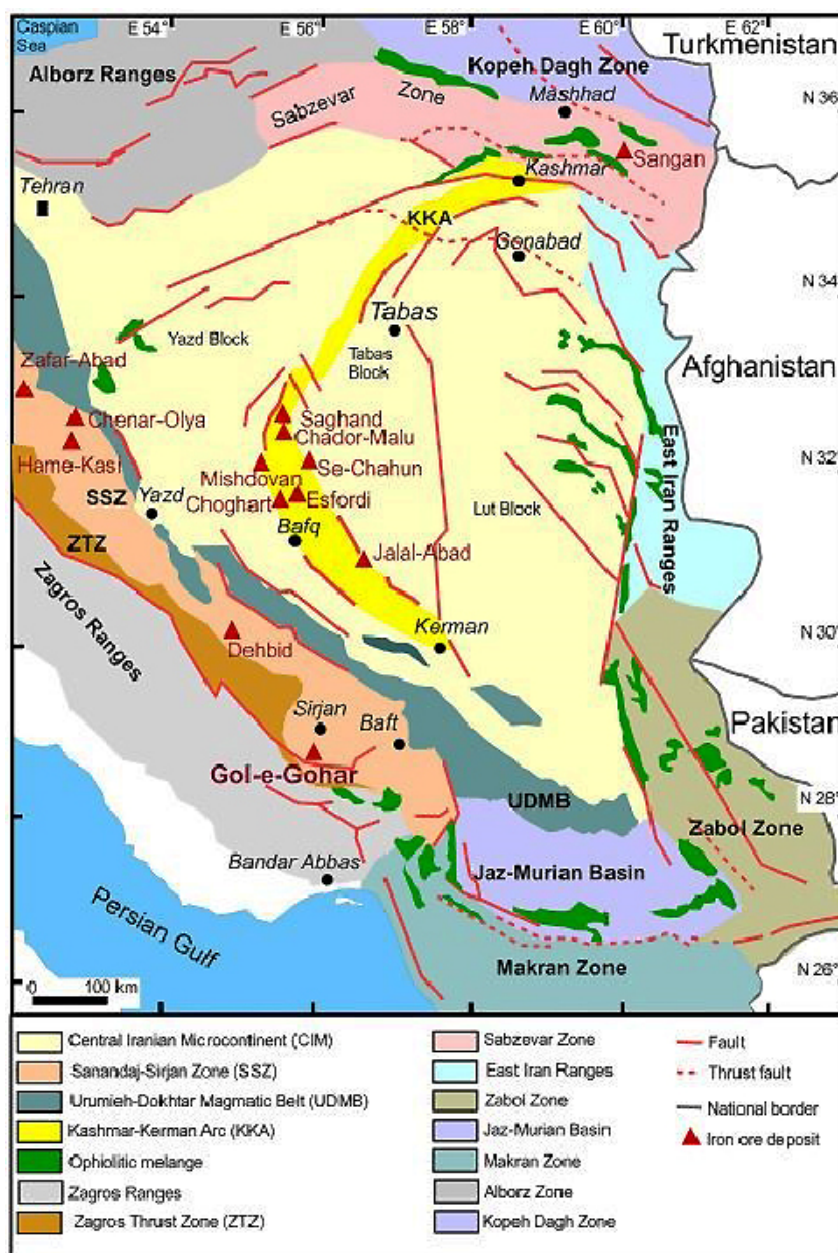
Figure 1. Structural map of Iran and location of the Gol-e-Gohar iron ore district within the Sanandaj-Sirjan zone
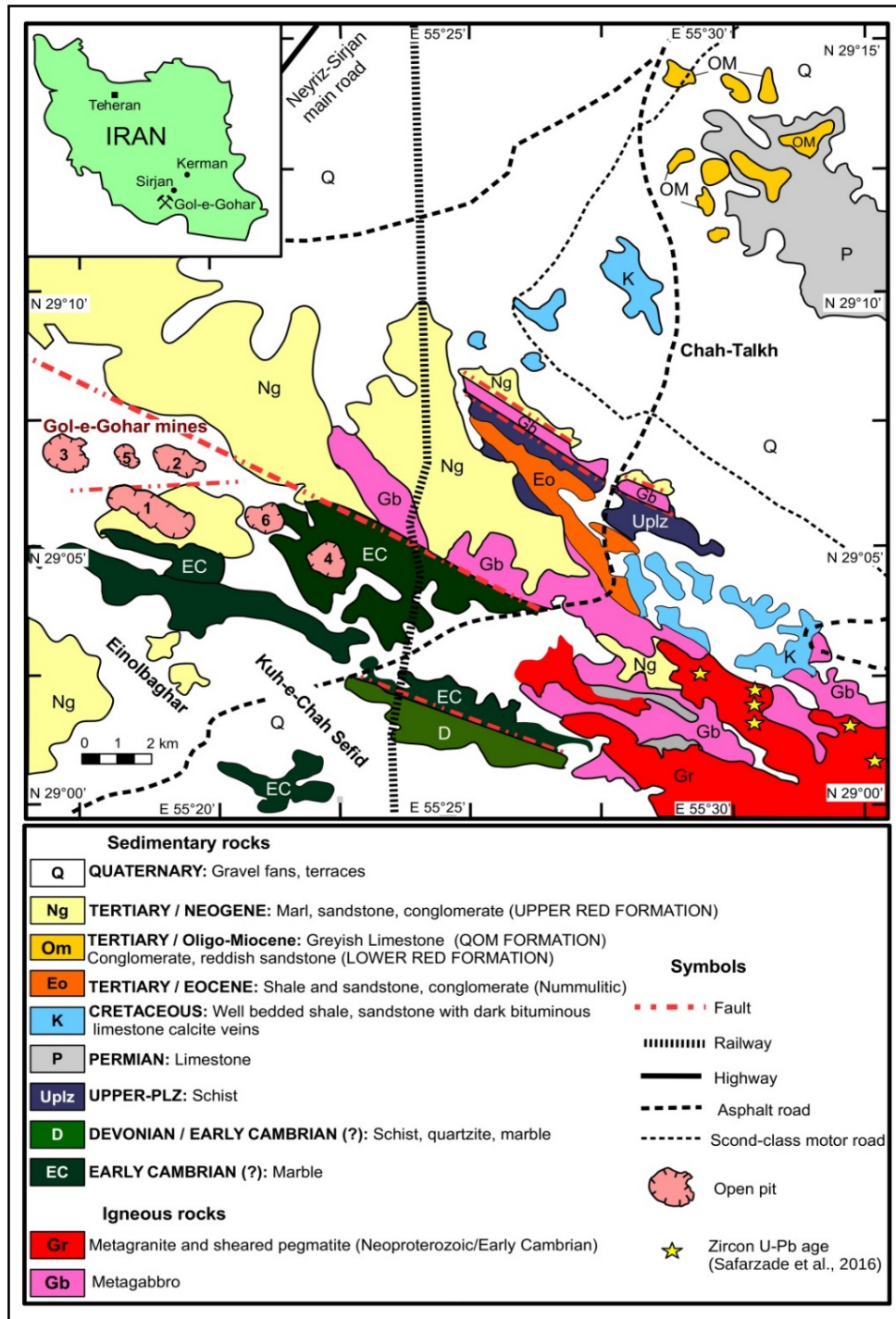
Figure 2. The Gol-e-Gohar region with the open pits/mines No. 1–6, and localities with U-Pb age data on zircon from Safarzade et al. (2016). Based on geological map of Neyriz quadrangle (1:250,000) (Sabzehei et al. (1993)

The largest deposit is Gol-e-Gohar No. 3 with about 643 Mt at a grade of 53.1% Fe (Eskandari, 2008). Phosphorus and sulfur contents of the ore are 0.11 wt% P and 0.76 wt% S, respectively (Badavi et al., 2019). The Gol-e-Gohar No. 3 deposit has a lenticular shape, about 2 × 2 km in diameter, up to about 100 m in thickness, and dips 30-45° toward the south. Field geology and mineralogy are described by Mirzaei et al. (2018) and Badavi et al. (2019).

Materials and methods

Thirty-one core samples from 10 drill holes were collected from the ore of the Gol-e-Gohar No. 3 deposit, and then 10 magnetite concentrate samples were selected and analyzed for major and trace elements by ICP-OES and ICP-MS techniques after lithium borate fusion and nitric acid digestion at ACME analytical laboratory in Vancouver, Canada. Some trace elements were analyzed after modified aqua regia digestion (1:1:1 HNO3: HCl: H2O) by ICP-MS at the same lab.

The Fe isotope composition of magnetite (4 samples from Gol-e-Gohar, plus 1 sample from Chador-Malu), pyrite (2 samples from Gol-e-Gohar), and hematite (1 sample from Esfordi) were determined by in situ femtosecond laser ablation multi-collector ICP-MS (LA-MC-ICP-MS) measurements at a high spatial resolution. All isotope ratios were determined on a Thermo Finnigan Neptune MC-ICP-MS instrument at the Leibniz University of Hannover, and corrected for the instrumental mass discrimination by using standard-sample-bracketing. The data are reported as δ^{56}Fe relative to the reference material IRMM-014 with a precision of 0.1‰ δ^{56}Fe. Triple oxygen isotope ratios (^{18}O/^{16}O) were determined for 9 magnetite samples from the Gol-e-Gohar iron deposit and for an additional two samples from the Esfordi and Chador-Malu mining district, using the analytical setup at the University of Göttingen, Germany. O2 was extracted from magnetite via laser-induced fluorination with BrF5 as the fluorinating agent. The sample gas was then cleaned from contaminant gases by distillation techniques and with a gas chromatograph, after which the isotope composition was measured using a MAT 253 mass spectrometer (Pack et al., 2016).

Results

Mineralogy and geochemistry of magnetite

The Gol-e-Gohar iron deposit consists mainly of magnetite, with minor alteration to hematite (Fig. 3G). Apatite is relatively rare (< 1 vol%) and intergrown with magnetite. The magnetite mineralization is followed by a sulfide stage with mainly pyrite, and minor chalcopyrite, and bornite. Locally, there is pyrrhotite intergrown with pyrite, and the pyrrhotite component is partly altered to marcasite (Fig. 3H). Pyrrhotite was possibly generated from the prograde decomposition of pyrite, and marcasite was likely generated from low-T retrograde alteration of pyrrhotite. Weathered samples contain limonite, hematite and goethite (Fig. 3). Under the microscope, the massive magnetite ore displays a granular and partly brecciated texture and consists of subhedral to anhedral grains of variable size (10–1000 μm). Locally, large euhedral grains of apatite (100–10000 μm) occur with fine inclusions of monazite (Fig. 3D). Sulfides are common and the most important sulfide phase is pyrite with variable size (1–1000 μm), shape, and abundance of inclusions. Pyrite is associated with rare fine-grained (< 100 μm) chalcopyrite, and pyrrhotite (Fig. 3). Nine magnetite concentrates and high-grade ore samples were analyzed by the same methods as for the whole rock samples (Table 1). The range of some elements in the magnetite concentrate are 0.97 ± 0.67 wt% SiO_2, 0.06 ± 0.05 wt% TiO_2, 0.19 ± 0.09 wt% Al_2O_3, 0.70 ± 0.34 wt% MgO, 0.46 ± 0.32 wt% CaO, 26.4 ± 20.6 ppm Co, 17 ± 5 ppm Cr, 27.0 ± 13.9 ppm Ga, 42.9 ± 39.3 ppm Ni, 17 ± 33 ppm Sn and 413 ± 367 ppm V.

Isotope geochemistry

Oxygen isotope composition of magnetite

The range of δ^{18}O values for nine magnetite samples ranging from 3.3 to 6.2‰ with an average δ^{18}O of +4.9 ‰, i.e., in good agreement with the range of magnetite δ^{18}O values for Gol-e-

Gohar that was reported by Bayati-Rad et al. (2011) ($3.8‰ \leq \delta^{18}O \leq 4.8‰$). Two magnetite samples from the Chador-Malu and Esfordi deposits that were analyzed for comparison have $\delta^{18}O$ values of 3.3 ‰ and 1.9 ‰, respectively (table 2).

Table 1. Chemical data (ICP and ICP-MS) for major and trace elements in magnetite concentrates from the Gol-e-Gohar iron deposit (major elements in wt%, trace elements in ppm, except Au in ppb).) (Mt Ore: Magnetite powder sample, Mt conc: Concentrated magnetite powder sample, DDH: Borehole Number with sampling depth)

Magnetite	B 8	D 3	E 2	F 6	F 8	H 5	I 5	J 3	Q 3	R 5
	Mt ore	Mt conc	Mt conc	Mt conc	Mt conc	Mt conc	Mt conc	Mt conc	Mt conc	Mt conc
	DDH 3019: 206m	DDH3 033:2 82m	DDH3 041:23 9m	DDH3 052:37 4m	DDH3 053:27 9m	DDH3 169:4 1m	DDH3 080:30 3m	DDH3 080:42 6m	DDH3 134:26 9m	DDH0 120:18 7m
SiO_2	2.89	1.04	0.59	2.58	0.57	1.16	0.70	0.54	0.34	1.18
TiO_2	0.01	0.05	0.15	0.11	0.08	0.06	0.04	0.01	0.02	0.03
Al_2O_3	0.16	0.31	0.19	0.38	0.11	0.19	0.13	0.21	0.12	0.11
ΣFe_2O_3	81.02	98.83	99.57	98.22	101.47	100.71	99.75	100.18	101.95	99.57
MgO	8.80	1.12	0.36	0.92	0.50	0.78	0.54	0.47	0.34	1.26
CaO	0.2	0.71	0.71	0.36	0.25	0.19	1.05	0.61	0.13	0.15
Na_2O	0.01	0.01	0.01	0.04	0.01	0.01	0.01	0.01	0.01	0.01
K_2O	0.01	0.01	0.01	0.01	0.01	0.01	0.01	0.01	0.01	0.01
P_2O_5	0.01	0.01	0.01	0.01	0.01	0.01	0.01	0.01	0.01	0.01
MnO	0.03	0.04	0.04	0.04	0.02	0.06	0.02	0.03	0.02	0.04
LOI	6.7	-2.3	-1.8	-2.9	-3.1	-3.2	-2.3	-2.1	-3	-2.4
Sum	99.82	99.78	99.79	99.81	99.91	99.96	99.89	99.95	99.92	99.92
TOT/C	0.12	0.20	0.18	0.02	0.12	0.02	0.26	0.26	0.06	0.06
TOT/S	1.54	0.02	0.02	0.08	0.10	0.08	0.64	0.44	0.22	0.44
Ag	0.1	0.1	0.1	0.1	0.1	0.1	0.1	0.1	0.1	0.1
As	13	1	1.2	0.8	1.4	2.3	5	1.1	2.6	1.1
Au	2.0	0.5	0.5	0.5	0.5	0.5	2.0	0.5	1.5	1.5
Ba	1	1	2	3	1	1	2	5	2	2
Be	1	1	1	1	1	1	1	1	1	1
Bi	0.1	0.1	0.1	0.1	0.1	0.1	0.1	0.3	0.1	0.2
Cd	0.1	0.1	0.1	0.1	0.1	0.1	0.1	0.1	0.1	0.1
Co	83.2	26.0	37.0	11.2	16.2	14.4	28.4	18.0	8.2	22.0
Cr	<14	21	14	21	<14	21	14	27	<14	14
Cs	0.1	0.1	0.1	0.1	0.1	0.1	0.1	0.1	0.1	0.1
Cu	54.4	5.2	3.2	43.6	6	10.7	89.1	9.8	19.8	49.7
Ga	0.5	36.7	39.7	44.2	31.4	3.9	30.2	27.5	37.7	23.1
Hf	0.1	0.2	0.1	0.1	0.1	0.2	0.1	0.1	0.1	0.1
Hg	0.01	0.01	0.02	0.01	0.01	0.01	0.01	0.03	0.02	0.01
Mo	0.1	0.5	0.6	0.1	0.1	0.1	0.2	0.1	0.4	0.1
Nb	0.5	0.1	0.1	0.6	1.2	0.5	0.8	0.5	0.5	0.5
Ni	1.3	28.2	30.5	136.4	19.1	2.0	57.7	57.5	21.2	33.3
Pb	0.5	0.5	1.4	0.6	1.1	1.3	1.7	3.2	1.2	2.8
Rb	0.1	0.1	0.1	0.4	0.1	0.1	0.1	0.3	0.1	0.1
Sb	0.6	0.3	0.6	0.2	0.3	0.7	0.7	1.3	0.4	0.3
Sc	1	2	1	1	2	2	2	2	2	1
Se	0.5	0.5	0.5	0.5	0.5	0.5	0.5	0.5	0.5	0.5
Sn	115	3	3	1	5	21	8	2	7	6
Sr	2.0	6	5.5	2.5	3	1.5	7.5	6.0	1.5	2.5
Ta	0.1	0.1	0.1	0.1	0.1	0.1	0.1	0.1	0.1	0.1
Th	0.4	0.9	0.2	1.8	0.8	0.3	0.2	0.2	0.2	0.2
Tl	0.1	0.1	0.1	0.1	0.1	0.1	0.1	0.1	0.1	0.1
U	1.6	1.6	0.9	0.4	1	0.9	0.2	0.3	0.3	0.1
V	8	976	1001	832	312	52	402	55	338	151

Y	0.5	0.5	0.2	1.8	0.1	0.6	0.7	2.8	0.4	0.2
Zn	16	30	27	27	35	24	28	33	21	40
Zr	4.4	7.2	1.6	1.6	1.2	4.5	1.2	1.6	1.7	1.2
La	0.2	0.5	0.3	2.8	0.3	0.4	0.8	0.7	0.2	0.2
Ce	0.2	0.7	0.2	6.7	0.4	0.5	0.7	0.7	0.2	0.3
Pr	0.02	0.02	0.02	0.78	0.02	0.02	0.02	0.05	0.02	0.02
Nd	0.3	0.3	0.3	3.3	0.3	0.3	0.3	0.6	0.3	0.3
Sm	0.05	0.05	0.05	0.05	0.05	0.05	0.05	0.05	0.05	0.05
Eu	0.02	0.02	0.02	0.06	0.02	0.02	0.02	0.02	0.02	0.02
Gd	0.06	0.10	0.05	0.45	0.05	0.15	0.10	0.15	0.15	0.05
Tb	0.01	0.01	0.01	0.06	0.01	0.02	0.01	0.03	0.02	0.01
Dy	0.05	0.05	0.05	0.30	0.05	0.15	0.10	0.20	0.05	0.05
Ho	0.02	0.02	0.02	0.06	0.02	0.04	0.02	0.06	0.02	0.02
Er	0.06	0.06	0.03	0.18	0.03	0.12	0.03	0.21	0.06	0.03
Tm	0.01	0.01	0.01	0.02	0.01	0.01	0.01	0.03	0.01	0.01
Yb	0.10	0.05	0.05	0.15	0.05	0.10	0.05	0.25	0.05	0.05
Lu	0.02	0.01	0.01	0.03	0.01	0.01	0.01	0.04	0.01	0.01

Table 2. Oxygen isotope data from the Gol-e-Gohar, Chador-Malu and Esfordi iron deposits.), $\delta^{18}O$ (‰):18O/16O isotopic ratio permil, 2 σ: 2*standard deviation

Sample	Mineral-Form	$\delta^{18}O$ (‰)	2 σ
3080: 426m	Mt-Powder	3.26	0.2
3070: 303m	Mt-Powder	4.57	0.2
3134: 269m	Mt-Powder	4.63	0.2
3041: 153m	Mt-Powder	3.79	0.2
3053: 278m	Mt-Powder	4.71	0.2
3032: 273m	Mt-Grain	6.19	0.2
3048: 258m	Mt-Grain	5.25	0.2
Gol-e-Gohar-3-3 (pit sample)	Mt-Grain	5.75	0.2
Gol-e-Gohar-3-1 (pit sample)	Mt-Grain	5.76	0.2
Chador-Malu, Iran	Mt-Grain	3.32	0.2
Esfordi, Iran	Mt-Grain	1.88	0.2

Iron isotope composition of magnetite and pyrite

Five polished sections were selected for Fe isotope analysis on magnetite and pyrite (29 points) (Table 3). The variation of iron isotope composition for magnetite (n = 17) is between 0.33 and 0.64 ‰ $\delta^{56}Fe$, with an average of 0.49 ± 0.05‰ $\delta^{56}Fe$. Pyrite (n = 12) displays a larger variation in Fe isotope composition from 0.74 to 1.39 ‰ and an average of 1.01 ± 0.19‰. In addition, two polished sections from the Chador-Malu deposit (magnetite, n = 5) and Esfordi (hematite, n = 6) were analyzed for comparison. The averages of iron isotope compositions for Chador-Malu and Esfordi, respectively, are 0.51 ± 0.04‰ and 0.48 ± 0.03‰.

Discussion

Geochemistry of magnetite

The composition of magnetite concentrates from the Gol-e-Gohar No. 3 iron deposit (Table 1: 9 samples plus a very magnetite-rich rock) are plotted in a number of discrimination diagrams. Fig. 4. A show the relatively low Ti concentration in the 100–1000 ppm range in the magnetite samples, combined with elevated Ni/Cr of mostly > 1, due to a chromium concentration of consistently ≤27 ppm.
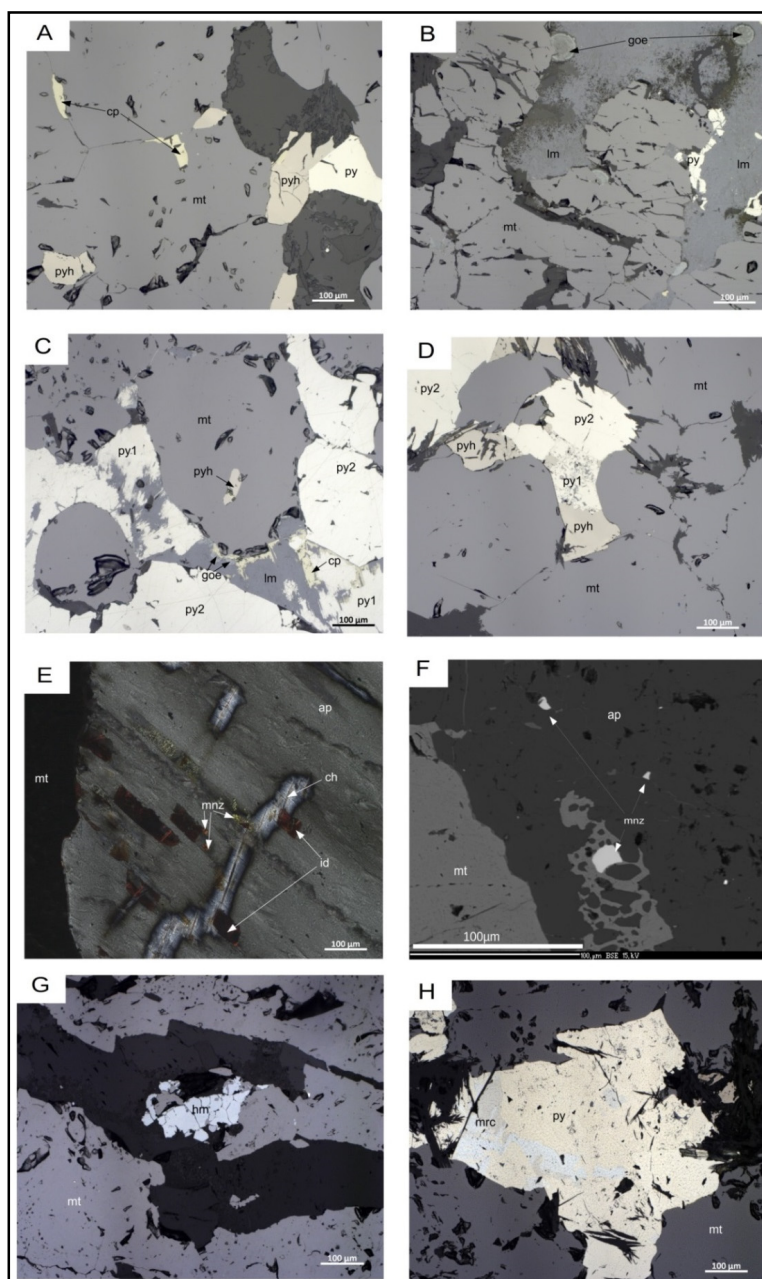
Figure 3. Photomicrographs in reflected light (RL, AD), in cross-polarized light (XPL, E) and by backscattered electrons (BSE. F) of ore minerals in the Gol-e-Gohar No. 3 iron deposit. The main ore mineral is magnetite (mt) with minor hematite (hm), associated with late-stage pyrite (py), pyrrhotite (pyh), chalcopyrite (cp). Pyrrhotite is intergrown with pyrite, and the pyrrhotite component is partly altered to marcasite. Weathering is expressed as goethite (goe) and limonite (lm). A) Magnetite as the main mineral and small grains of iron sulfides (pyrite, chalcopyrite and pyrrhotite), (DDH 3020: 251–258 m). B) Magnetite affected by alteration to limonite and goethite with spherulitic structure (DDH 3020: 220–228 m). C) and D) Granoblastic magnetite (mt) with late-stage pyrite (py), chalcopyrite (cp), pyrrhotite (pyh). The most important iron ore minerals are displayed in this sample (i.e., magnetite, pyrite, chalcopyrite, pyrrhotite, limonite and goethite). Pyrrhotite is intergrown with pyrite, and the pyrrhotite component is partly altered to marcasite, likely from low-T retrograde alteration of pyrrhotite (DDH 3059: 252–258 m and DDH 3020: 251–258 m). E) and F) Big euhedral apatite inside magnetite with very fine grains of monazite ((X6: inside pit). G) Magnetite with minor alteration to hematite (DDH 3032: 264 m). H) Pyrite and marcasite with relics of pyrrhotite (DDH 3020: 251–258 m). mt: magnetite, hm: hematite, py: pyrite, pyh: pyrrhotite, cp: chalcopyrite, mrc: marcasite, goe: goethite, lm: limonite, mnz: monazite

Table 3. Iron isotope data from the Gol-e-Gohar, Chador-Malu and Esfordi iron ore deposits (Mt: Magnetite, Py: pyrite, Hm: hematite polished sample, DDH: Borehole Number with sampling depth), δ56Fe (‰):56Fe/54Fe isotopic ratio permil, 2 σ: 2*standard deviation

Sample	Mineral	δ56Fe (‰)	2 σ
Gol-e-Gohar-3-1 (pit sample)	Mt	0.60	0.05
	Mt	0.61	0.05
	Mt	0.61	0.04
	Mt	0.44	0.05
	Mt	0.50	0.04
Gol-e-Gohar-3-3 (pit sample)	Mt	0.51	0.04
	Mt	0.33	0.04
	Mt	0.34	0.04
	Mt	0.64	0.04
DDH 3032: 273m	Mt	0.58	0.04
	Mt	0.60	0.04
	Mt	0.42	0.05
	Mt	0.47	0.05
	Mt	0.47	0.05
	Mt	0.42	0.06
DDH 3048: 258m	Mt	0.43	0.06
	Mt	0.34	0.05
	Py	1.34	0.05
	Py	1.39	0.05
	Py	1.35	0.05
	Py	1.38	0.05
	Py	0.94	0.05
	Py	0.76	0.05
	Py	0.90	0.05
DDH 3032: 264m	Py	0.60	0.06
	Py	0.90	0.07
	Py	0.74	0.07
	Py	0.82	0.07
	Py	1.05	0.07
	Mt	0.46	0.05
	Mt	0.51	0.05
Chador-Malu, Iran	Mt	0.54	0.05
	Mt	0.47	0.05
	Mt	0.56	0.04
	Hm	0.46	0.05
	Hm	0.45	0.05
Esfordi, Iran	Hm	0.58	0.05
	Hm	0.49	0.05
	Hm	0.54	0.05
	Hm	0.44	0.04

Magnetite with Cr < 100 ppm and V > 500 ppm is typical of Kiruna-type mineralization (Knipping et al., 2015a, 2015b). These features indicate an origin from hydrothermal fluids where the solubility of Ni and V is higher than for Cr, and lower than for Ti. Nevertheless, a few samples have Ni/Cr about 0.1, which could be interpreted as an igneous feature. The mixed igneous-hydrothermal pattern is also visible in some other parameters, such as V content with a large range of 50–1000 ppm, or Ga content with a range from 4 to 44 ppm.

One sample from very magnetite-rich rock has elevated Sn (115 ppm), very low V (8 ppm), very low Ni (1.3 ppm), very low Ga (0.5 ppm), but elevated Co (83 ppm). The magnetite in this sample could have a hydrothermal origin. A particular feature is the Sn content which was also seen in some silicate rock samples, indicating a granite-related hydrothermal system. In terms of a variety of discriminating parameters, the Gol-e-Gohar magnetite samples plot variably in the Kiruna-type, IOCG, and porphyry fields, and are indicative of a high-temperature origin.
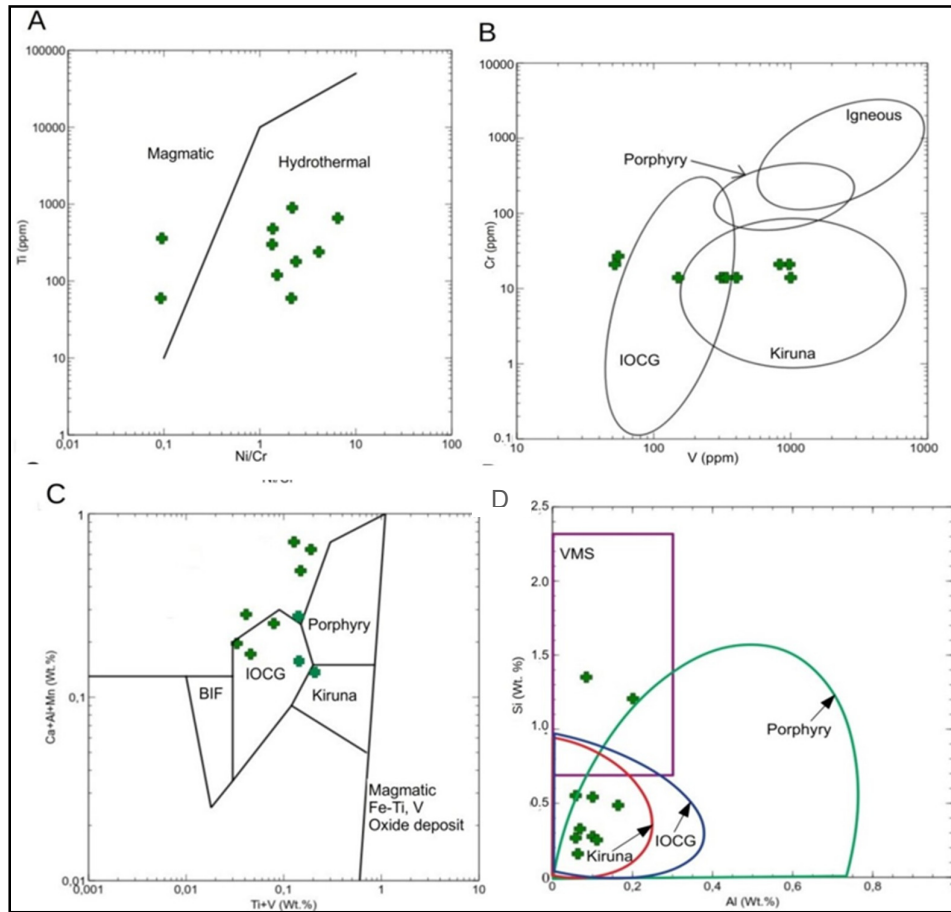
Figure 4. Chemical discrimination diagrams for magnetite in the Gol-e-Gohar iron deposit. A) Ti vs Ni/Cr ratio in magnetite (Mt) to distinguish magmatic and hydrothermal settings (Dare et al., 2014). Magnetite from Gol-e-Gohar plots in the hydrothermal field. B) Cr vs. V diagram (Knipping et al., 2015a, 2015b). Magnetite from Gol-e-Gohar plots in the Kiruna-IOCG field. C) Ca + Al + Mn vs. Ti + V diagram showing average compositions of Gol-e-Gohar magnetite (ICPMS data), after Dupuis and Beaudoin (2011). Magnetite from Gol-e-Gohar plots in the IOCG field. D) Si vs Al diagram, after Lohberg and Horndhal (1983). Low value of Si and Al in the magnetite of Gol-e-Gohar is typical of Kiruna type

The element variability in the Gol-e-Gohar is likely related to varying temperature, due to the wide range of Ti, V, and Cr in the magnetite samples. The magnetite samples from Gol-e-Gohar show higher Ca + Al + Mn and Ti + V concentrations than those from BIFs, and mostly lower concentrations than in porphyry and igneous systems (Fig. 4.C and D). Magnetite has relatively low Ni (38 ± 39 ppm), Co (26 ± 21 ppm), Zn (29 ± 6 ppm), MnO (0.03 ± 0.01 wt%), SiO_2 (0.97 ± 0.67 wt%), and Al_2O_3 (0.19 ± 0.09 wt%) but slightly elevated Sn (17 ± 33 ppm) which may point to a felsic igneous source, similar to typical Kiruna deposits (Lohberg & Horndhal, 1983; Nadoll et al., 2014; Fig. 4. E and F).

Comparison of geochemical results on the magnetite in Gol-e-Gohar and Chador-Malu deposits

The geochemical data of magnetite in The Gol-e-Gohar No. 3 iron deposit are compared with the data obtained from magnetite of Chador-Malu mine (Torab, 2008 and Torab & Lehman 2007). The average abundance of important elements of these two deposits is given in Table 4.

Figure 5, with different diagrams, shows the position of the magnetites in these two deposits and the clear similarities between the two deposits.

The next section (isotopic evidence) provides the better reasons to confirm the genetic similarities between these two deposits.

According to Table 2, the amounts of aluminum and titanium in the two anomalous iron deposits (No. 3 of Gol-e-Gohar and Chador-Malu) are close to each other, while the amounts of vanadium, chromium and cobalt in the Gol-e-Gohar magnetite are much lower than the values reported from Chador-Malu magnetite. The high amounts of the above elements indicate a higher temperature for the formation of magnetites in Chador-Malu deposit than the magnetites in Gol-e-Gohar iron deposit. Nickel value in the Gol-e-Gohar magnetite is 13.9 ± 11.9 g / ton, which is much lower than its value in Chador-Malu magnetite (99.6 ± 191.2 g / t). In Figure 5, A, the positions of Chador-Malu and Gol-e-Gohar magnetites are located in the hydrothermal area, while the position of Chador-Malu is closer to the magmatic area. In Figures 5, B and C, due to the higher amounts of vanadium, titanium and nickel in the magnetite of Chador-Malu iron deposit, this deposit is more inclined to igneous origin type. Despite these slight differences, magnetites from both deposits are located in the hydrothermal origin area. Based on Figure 5D, the magnetites from No. 3 Gol-e-Gohar iron deposit are located in the IOCG area and Chador-Malu magnetites are more inclined to Kiruna type, which of course is not much different. So, both deposits are originally from a high-temperature magmatic-hydrothermal fluid, which are considered to be related to the early Paleozoic felsic magmatism (host metagranites). According to Singoyi et al. (2006) and Dupuis & Beaudoin (2011), it clearly shows the similarity of mineralization in Gol-e-Gohar iron deposit to Kiruna type. By Comparing of trace elements in the Gol-e-Gohar magnetite and checking their distribution pattern with other iron deposits of Iran, it shows the most similarity between Gol-e-Gohar iron deposit and deposits of Central Iran, especially the Chador-Malu deposit (Bafgh). The only difference is that the Bafgh iron deposit is formed at a higher temperature and closer to magmatic type (but still kiruna type), (Torab, 2007).

Table 4. The average chemical composition of magnetite in Gol-e-Gohar and Chador-Malu deposits (Σ:Variation range)

Samples	Gol-e-Gohar, Iran	Chador-Malu, Iran
Properties	Type: Kiruna, Data: This study	Kiruna, Data: (Torab, 2007)
Al_ppm	233	130
Σ	±56.8	±79.1
Ti_ppm	63.3	120.0
Σ	±54.9	0.0
V_ppm	3.6	2581.1
Σ	±2.9	±1204.7
Ni_ppm	11.9	191.2
Σ	±13.9	±99.6
Co_ppm	8.6	Non
Σ	±5.4	Non
Zn_ppm	42.8	Non
Σ	±17.8	Non
Ga_ppm	2.3	Non
Σ	±2.1	Non
Nb_ppm	0.1	Non
Σ	±0.1	Non
Sn_ppm	20.5	Non
Σ	±10.2	Non
Ta_ppm	0.003	Non
Σ	±0.003	Non

Oxygen isotopes

In Figure 6, we compare the δ^{18}O values of magnetite from Gol-e-Gohar with the δ^{18}O values of magnetite from other iron deposits. The δ^{18}O of magnetite from Gol-e-Gohar is similar to magnetite from the Pilot Knob iron deposit, USA (3.3 ≤ δ^{18}O ≤ 6.7‰), which could be related to magmatic-hydrothermal fluids in equilibrium with a silicate melt (Childress et al., 2016). The δ^{18}O of magnetite from Gol-e-Gohar is similar, although slightly elevated, compared to the well-known iron ore deposits in central Iran (Chador-Malu and Esfordi).

Fe isotopes

The global range for igneous magnetite is 0.06–0.49‰ δ^{56}Fe (Heimann et al., 2008; Weis, 2013), and the general range for high-temperature magmatic-hydrothermal magnetite is 0.06–0.86‰ δ^{56}Fe (Bilenker et al., 2016). The Gol-e-Gohar iron deposit has a range between 0.33 and 0.64‰ δ^{56}Fe, with an average of 0.49 ± 0.05‰ δ^{56}Fe (Table3).
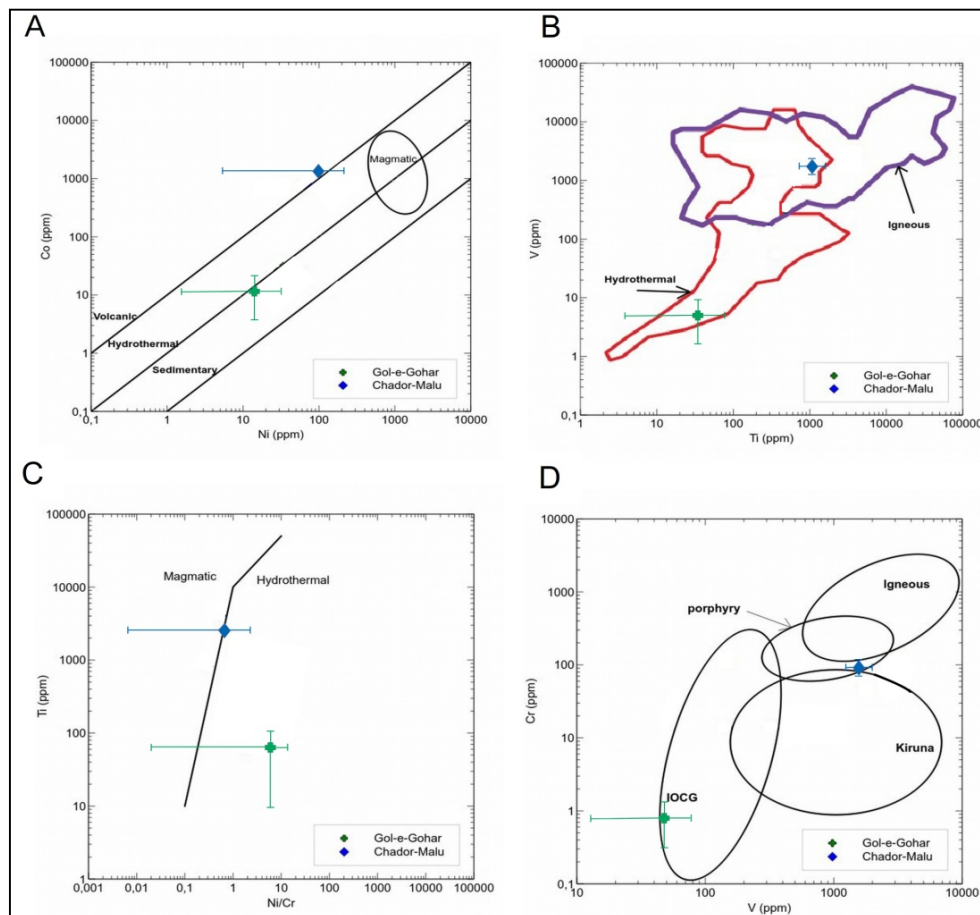
Figure 5. Geochemical diagrams of magnetite in No.3 Gol-e-Gohar iron deposit in comparison with the chemical composition of Chador-Malu iron deposit, A) Ni vs Co diagram (Nadoll et al., 2014). Gol-e-Gohar Sirjan and Chador-Malu magnetites are both located in the range of hydrothermal deposits with a slightly greater tendency of Chador-Malu deposit to the magmatic deposits; B) V vs Ti diagram (Dare et al., 2014a); C) Ti vs Ni / Cr diagram. B) and C) diagrams are distinguishing magmatic and hydrothermal origins. The magnetites from the both districts are located in hydrothermal origin. Chador-Malo samples also overlap with igneous magnetites; D) Cr vs. V diagram (Knipping et al., 2015a, b). The samples of Gol-e-Gohar Sirjan iron ore deposit are plotted in the IOCG area and the samples of Chard-Malu are plotted in the area of Kiruna

The comparison of these data with those from some other iron ore deposits (Fig. 7) identifies the Gol-e-Gohar iron deposit as of high-T magmatic-hydrothermal origin, similar to Chador-Malu and Esfordi, and with slightly more elevated δ^{56}Fe than the Kiruna, Pilot Knob and El Laco deposits.
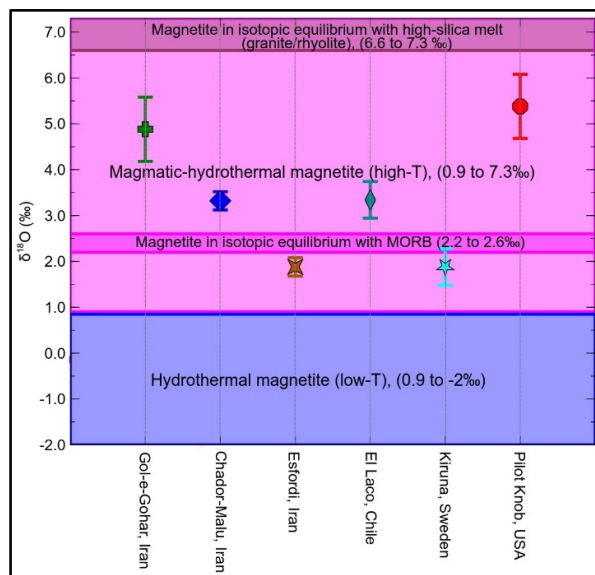
Figure 6. Oxygen isotope (δ^{18}O) ratios in magnetite from the Gol-e-Gohar iron deposit (this study) compared to those for other iron deposits, i.e. Chador-Malu and Esfordi, (Iran; this study), El Laco (Chile; Bilenker et al., 2016), Kiruna (Sweden; Weis, 2013) and Pilot Knob (USA; Childress et al., 2016). Data are listed in Table 5. Light pink colored band (δ^{18}O = 0.9–7.3‰) represents the general range for magmatic-hydrothermal magnetite (high-temperature) (Taylor, 1967, 1968). This range includes magnetite that is in isotopic equilibrium with mid-ocean ridge basalt (MORB; δ^{18}O = 2.2–2.6‰), and magnetite in isotopic equilibrium with high-silica melt (granite/rhyolite; δ^{18}O = 6.6–7.3‰). The line with δ^{18}O = 0.9‰ corresponds to the suggested value for discriminating between magmatic-hydrothermal magnetite (high-T) and low-temperature hydrothermal magnetite (Jonsson et al., 2013)
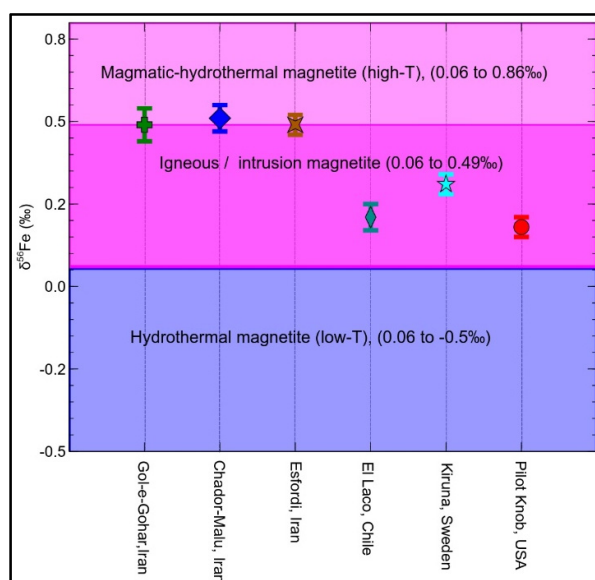
Figure 7. Iron isotope composition (δ^{56}Fe) for magnetite from the Gol-e-Gohar iron deposit compared to other iron deposits, i.e. Chador-Malu and Esfordi (Iran; this study), El Laco (Chile; Bilenker et al., 2016), Kiruna (Sweden; Weis, 2013) and Pilot Knob (USA; Childress et al., 2016). Data are taken from Table 6. The global range for igneous magnetite is δ^{56}Fe = 0.06–0.49‰ and the general range for magmatic-hydrothermal (high-T) magnetite is δ^{56}Fe = 0.06–0.86‰ (adapted from Bilenker et al., 2016)

Table 5. Oxygen isotope data from the Gol-e-Gohar, Chador-Malu and Esfordi iron ore deposits and elsewhere in world (Mt: Magnetite samples, δ ^{18}O (‰):$^{18}O/^{16}O$ isotopic ratio permil. 2 σ: 2*standard deviation)

Sample/Locality	Mineral	δ ^{18}O(‰)	2 σ	Literature data
Gol-e-Gohar (n=9)		4.88	0.70	This study
Gol-e-Gohar (n=5)	Mt	4.14	1.05	Bayati Rad, et al., 2011
Chardor-Malu, Iran		3.32	0.20	This study
Esfordi, Iran		1.88	0.20	This study
		2.41	0.02	
		3.04	0.05	
		2.75	0.04	
		3.17	0.03	
		2.36	0.04	
		6.18	0.12	
El Laco, Chile	Mt	6.74	0.12	Bilenker et al., 2016
		2.99	0.10	
		2.78	0.03	
		2.48	0.03	
		2.04	0.03	
		4.00	0.10	
		4.34	0.10	
		1.49	0.04	
		1.20	0.20	
		1.80	0.20	
		0.90	0.20	
		2.80	0.20	
		1.20	0.20	
Kiruna, Sweden	Mt	1.10	0.20	Weis, 2013
		1.00	0.20	
		1.20	0.20	
		1.80	0.20	
		1.50	0.20	
		7.90	0.20	
		0.20	0.20	
		3.26	0.08	
Pilot Knob, USA	Mt	6.68	0.08	Childress et al., 2016
		6.21	0.06	

Table 6. Iron isotope data from the Gol-e-Gohar, Chador-Malu and Esfordi iron ore deposits and elsewhere in world (Mt: Magnetite samples, $\delta^{56}Fe$ (‰):$^{56}Fe/^{54}Fe$ isotopic ratio permil. 2 σ: 2*standard deviation)

Sample/Locality	Mineral	δ ^{56}Fe (‰)	2 σ	Literature data
		0.22	0.03	
		0.09	0.06	
		0.22	0.03	
		0.14	0.08	
		0.13	0.05	
		0.08	0.03	
		0.21	0.07	
		0.12	0.03	
El Laco, Chile	Mt	0.1	0.06	Bilenker et al., 2016
		0.22	0.05	
		0.14	0.02	
		0.18	0.03	
		0.18	0.07	
		0.22	0.03	
		0.24	0.08	
		0.18	0.03	

Sample/Locality	Mineral	δ^{56}Fe (‰)	2 σ	Literature data
		0.39	0.09	
		0.29	0.03	
		0.3	0.03	
		0.32	0.09	
		0.53	0.03	
		0.27	0.03	
		0.2	0.03	
		0.13	0.03	
		0.4	0.03	
		0.24	0.03	
		0.33	0.03	
		0.31	0.03	
		0.31	0.04	
Kiruna, Sweden	Mt	0.3	0.04	Weis, 2013
		0.26	0.04	
		0.29	0.03	
		0.39	0.04	
		0.27	0.04	
		0.31	0.03	
		0.27	0.04	
		0.19	0.03	
		0.24	0.04	
Pilot Knob, USA	Mt	0.14	0.05	Childress et al., 2016
		0.18	0.03	
		0.06	0.05	
		0.27	0.06	

Conclusions

Petrographic features and stable isotope data (iron and oxygen) document the importance of magmatic-hydrothermal processes in the genesis of the Gol-e-Gohar iron deposit. Magnetite crystallized from a magmatic-hydrothermal (high-T) fluid of a granitic source. The trace-element chemical composition of the Gol-e-Gohar magnetite suggests a Kiruna or IOCG affiliation, and the broad elemental variability is likely because of variation in temperature during the mineralization.

Acknowledgments

References

Badavi, M., Atapour, H., Mohammadi, M., 2019. Mineralogy, petrography, geochemistry of magnetite ore and sulfide minerals and the possible model of mineralization at Anomaly #3, Gol-e-Gohar, iron mine, Sirjan (Kerman). Petrology 38: 49-79 (in Persian with English Abstract).
Bayati-Rad, Y., Mirnejad, H., Ghalamghash, J., 2011. Evaluating the origin of magnetite and sulfide

phases from Gol-Gohar iron ore deposit (Sirjan): constraints from O and S isotope data. Geosciences 20: 139-146.

Bayati-Rad, Y., Mirnejad, H., Ghalamghash, J., 2013. Distribution and abundance of rare earth elements in magnetite from Gol-Gohar iron ore deposit, Sirjan-Kerman. Sci. Q. J. Geosciences 23 (90): 217-224.

Bilenker, L.D., Simon, A.C., Reich, M., Lundstrom, C.C., Gajos, N., Bindeman, I., Barra, F., Munizaga, R., 2016. Fe-O Stable isotope pairs elucidate a high-temperature origin of Chilean iron oxide-apatite deposits. Geochimica et Cosmochimica Acta 177: 94-104.

Childress, T.M., Simon, A.S., Day, W.C., Lundstrom, C.C., Bindeman, I.N., 2016. Iron and oxygen isotope signatures of the Pea Ridge and Pilot Knob magnetite-apatite deposits, Southeast Missouri, USA. Economic Geology 111: 2033-2044.

Dare, S.A., Barnes, S.J., Beaudoin, G., Méric, J., Boutroy, E., Potvin-Doucet, C., 2014a. Trace elements in magnetite as petrogenetic indicators. Mineralium Deposita 49: 785-796.

Dupuis, C., Beaudoin, G., 2011. Discriminant diagrams for iron oxide trace element fingerprinting of mineral deposit types. Mineralium Deposita 46: 1-17.

Evans, B.W. and Frost, B.R., 1975. Chrome-spinel in progressive metamorphism-preliminary analysis. Geochimica et Cosmochimica Acta, 39: 959-972.

Heimann, A., Beard, B.L., Johnson, C.M., 2008. The role of volatile exsolution and sub-solidus fluid/rock interactions in producing high ^{56}Fe/ ^{54}Fe ratios in siliceous igneous rocks. Geochimica et Cosmochimica Acta, 72: 4379-4396.

Jonsson, E., Troll, V.R., Högdahl, K., Harris, C., Weis, F., Nilsson, K.P., Skelton, A., 2013. Magmatic origin of giant 'Kiruna-type' apatite-iron-oxide ores in Central Sweden. Scientific Reports 3: 16-44.

Knipping, J.L., Bilenker, L.D., Simon, A.C., Reich, M., Barra, F., Deditius, A.P., Lundstrom, C., Bindeman, I., Munizaga, R., 2015a. Giant Kiruna-type deposits form by efficient floation of magmatic magnetite suspensions. Geology 43: 655-656.

Knipping, J.L., Bilenker, L.D., Simon, A.C., Reich, M., Barra, F., Deditius, A.P., Lundstrom, C., Bindeman, I., Munizaga, R., 2015b. Trace elements in magnetite from massive iron oxide-apatite deposits indicate a combined formation by igneous and magmatic-hydrothermal processes. Geochimica et Cosmochimica Acta, 171: 15-38.

Loberg, B.E.H., Horndhal, A.K., 1983. Ferride geochemistary of swedish Precambrian iron ores. Mineralium deposita, 18: 478-504.

Mirzaei, A., Ahmadi, A., Mirnejad, H., Gao d, J.F., Nakashima, K. and Boomeri, M., 2018. Two-tiered magmatic-hydrothermal and skarn origin of magnetite from Gol-Gohar iron ore deposit of SE Iran: In-situ LA–ICP-MS analyses. Ore Geology Reviews, 102: 639-653.

Mohajjel, M. Fergusson, C.L., 2000. Dextral transpression in Late Cretaceous continental collision Sanandaj-Sirjan zone western Iran. Journal of Structural Geology 22: 1125-1139.

Mohajjel, M. Fergusson, C.L. and Sahandi, M.R., 2003. Cretaceous–Tertiary convergence and continental collision, Sanandaj–Sirjan Zone, western Iran. Journal of Asian Earth Sciences 21: 397-412.

Mücke, A. and Golestaneh, F., 1982. The genesis of the Gol Gohar iron ore deposit (Iran). Chemie der Erde - Geochemistry, 41(3): 193-212.

Nadoll, P. Angerer. T. Mauk, J. L. French, D., Walshe, J., 2014a.The chemistry of hydrothermal magnetite. A review. Ore Geology Reviews, 61: 1-32.

Ramezani J., and Tucker, R.D., 2003. The Saghand region, Central Iran: U-Pb geochronology, petrogenesis and implications for Gondwana tectonics: American Journal of Science, 303: 622-665.

Safarzade, E., Masoudi, F., Hassanzade, J. and Pourmoafi, S.M., 2016. The presence of Precambrian basement in Gol-e-Gohar of Sirjan (south of Iran). Petrology 26: 153-170.

Sheikholeslami, M.R., Pique, A., Mobayen, P., Sabzehei, M., Bellon, H., Emami, H., 2008. Tectono-metamorphic evolution of the Neyriz metamorphic complex, Quri-Kor-eSefid area (Sanandaj-Sirjan Zone, SW Iran). J. Journal of Asian Earth Sciences, 31: 504–521.

Singoyi, B., Danyushevsky, L., Davidson, G.J., Large, R., Zaw, K., 2006. Determination of trace elements in magnetites from hydrothermal deposits using the LA-ICP-MS technique. Abstracts of Oral and Poster Presentations from the SEG, Conference Society of Economic Geologists, Keystone, USA, 367-368.

Taylor, H.P. Jr., 1967. Oxygen isotope studies of hydrothermal mineral deposits, in Barnes, H.L., ed.,

Geochemistry of Hydrothermal Ore Deposits. New York, Holt, Rinehart and Winston, 109-142.

Taylor, H.P. Jr., 1968. The oxygen isotope geochemistry of igneous rocks. Contributions Mineralogy and Petrology 19: 1-71.

Torab, F. M., 2008. Geochemistry and metallogeny of magnetite-apatite deposits of the Bafq Mining District, Central Iran. Doctoral Thesis, Clausthal University of Technology, 131 p.

Torab, F.M., Lehmann, B., 2007. Magnetite-apatite deposits of the Bafq mining district, Central Iran: apatite geochemistry and monazite geochronology. Mineralogical Magazine 71: 347-363.

Weis, F., 2013. Oxygen and iron isotope systematics of the Grängesberg mining district (GMD), Central Sweden. M.S. thesis, Uppsala University, 77 p.

Young, G.M., 1976. Iron-formation and glaciogenic rocks of the Rapitan Group, Northwest Territories, Canada. Precambrian Research, 3: 137-158.